Eurasian Journal of Science and Technology

2024, Volume 4, Issue 4

Original Research Article

Enhanced Energy Bandgap, Structural, and Electrical Conductivity of Electrochemically Synthesized FeSe Nanostructured Material for Photovoltaic Applications

Ernest O. Ojegu[1]| Okpara Natheniel[1] | Imosobomeh L. Ikhioya[2,*]

[1]*Department of Physics, Delta State University, Abraka. Delta State, Nigeria*
[2]*Department of Physics and Astronomy, University of Nigeria, Nsukka, 410001, Enugu State, Nigeria*

Use your device to scan and read the article online

Citation E. O. Ojegu, O. Natheniel, I. L. Ikhioya, **Enhanced Energy Bandgap, Structural, and Electrical Conductivity of Electrochemically Synthesized FeSe Nanostructured Material for Photovoltaic Applications.** *Eurasian J. Sci. Technol.*, **2024**, *4*(4), 355-365.

https://doi.org/10.48309/EJST.2024.453710.1137

Article info:
Received: 2024-04-22
Accepted: 2024-05-27
Available Online: 2024-06-02
ID: EJST-2404-1137
Checked for Plagiarism: Yes
Checked Language: Yes

Keywords:
FeSe, Bandgap, Optical, Structural, Resistivity, Conductivity

ABSTRACT

FeSe material was synthesized using the electrochemical deposition technique. The Iron nitrate nonahydrate ($Fe(NO_3)_2.9H_2O$) is a part of the electrochemical bath system. FeSe material exhibits a diffraction value of 14.372o at 2θ. The diffraction peaks at 2θ = 14.372°, 15.027°, 19.112°, 23.575° 26.623° 32.292°, and 34.242° correspond, respectively, to the diffraction planes of 011, 101, 111, 112, 200, 211, and 212 of FeSe material. The results showed that longer deposition time resulted in lower resistivity and higher conductivity. Longer deposition times lead to an increase in the thickness and grain size of the FeSe films, which can affect the electronic band structure. Iron selenide material showed a direct transition bandgap ranging from 2.10 to 1.65 eV at deposition times of 5 to 20 seconds. The resistivity and conductivity of FeSe thin films was synthesized at various deposition times (5-20 seconds). The results showed that longer deposition time resulted in lower resistivity and higher conductivity. The reflectance increases as the deposition time increased. Iron selenide material showed a direct transition bandgap ranging from 2.10 to 1.65 eV at deposition times of 5 to 20 seconds.

Introduction

The extensive study of transition metal chalcogenides is driven by their unique electronic properties, which make them suitable for various applications. Their unique electronic properties drive the extensive study of transition metal chalcogenides [1-3], as they are suitable for various applications such as being used as photo-absorbers in photovoltaics, non-linear optical materials in bio-imaging, cathode materials in lithium-air batteries, and anode materials in sodium-ion batteries. Their recent demonstration highlighted their significant role as electro catalysts in various reactions, including oxygen and hydrogen evolution and water splitting. FeSe attracted significant attention due to its potential as a solar cell absorber, especially following the discovery of superconductivity in this group of compounds [3-7]. Different methods as pulsed

*Corresponding Authors: Imosobomeh L. Ikhioya (imosobomeh.ikhioya@unn.edu.ng)

laser deposition, molecular beam epitaxy, and chemical vapor deposition, are used to grow FeSe films. While these methods have been crucial for studying material properties, they are not suitable for growing larger samples or for industrial scale-up. Electrodeposition offers multiple advantages compared to the previously mentioned thin-film deposition methods [8-12]. Unlike thermal processes, one can perform this at room temperature and ambient pressure. The process can create complex, curved films that are large, thick, and uniform. Inexpensive equipment and standard lab conditions make scaling up easy. Other techniques like MBE, PLD, or CVD cannot achieve the same deposit's crystalline quality and microstructure [13-17]. Several authors have investigated the possibility of using electrodeposition to grow, for purposes such as superconducting tapes or dye-sensitized solar cells. Researchers have been particularly intrigued by FeSe, an Fe-based superconductor, as it exhibits remarkable and intricate physical properties within its simplest crystal structure. Ubale *et al.* [16] used the chemical bath deposition technique to deposit iron selenide thin films onto glass substrates. X-ray diffraction and Fourier transforms infrared spectrum were used to structurally characterize iron selenide thin films. The morphology of FeSe thin film was characterized using scanning electron microscopy and atomic force microscopy.

The results show that nano-rectangular rods and plates led to a porous grain structure. During deposition, the thin films exhibited optical band gap energy of 2.60 eV. Initially deposited, the FeSe thin films show p-type electrical conductivity and behave like semiconductors. The room's electrical resistivity is around 1.1×10^5 Ω-cm at low temperatures, and it has activation energy of 0.26 eV. FeSe films were prepared on CaF_2, LiF, and $SrTiO_3$ substrates by Wang *et al.* [17] using the pulsed laser deposition (PLD) technique and identical growth parameters were able to measure the superconducting transition temperatures of the samples by placing electrodes on the film surfaces. The recorded temperatures were 11.44 K, 10.91 K, and 5.4 K. Raman spectra showed two phonons (A1g, B1g) from different samples, suggesting varied strain effects from the substrates. A dispersion model was established, incorporating Lorentz + Drude oscillations, to accurately represent the properties of FeSe films. The analysis of physical properties, including complex refractive index and scattering rate, was performed using spectroscopic ellipsometry (SE) inversion. The standard critical point (SCP) model was utilized to fit the second derivatives of the imaginary part of the dielectric function and determine the transition energy. The physical origin of the transition peaks was determined by combining first-principles calculations based on DFT. Using this as a foundation, they introduce a fresh technique for obtaining the FeSe pseudo-gap by analyzing the disparity in SE transition energies. According to the experimental results, there is an inverse relationship between the pseudo-gap of FeSe film and the superconducting transition temperature.

The process of electrochemical deposition depends on redox reactions occurring within an electrochemical cell. The components of an electrochemical cell include an electrolytic bath and three electrodes: a working electrode, a counter electrode, and a reference electrode. The reference electrode ensures a stable ground voltage, crucial for precise electrochemical potential measurement. The reference electrode is placed close to the working electrode for measuring its potential relative to the stable reference electrode [18-28]. The standard hydrogen electrode defines the equilibrium between H^+ and H_2 gas as zero utilizing more convenient reference electrodes such as Ag/AgCl or Hg_2Cl_2. The electrode potential is vital for controlling electron and ion transfer in chemical reactions on electrodes. The chemical processes are controlled by the voltage and current flowing through the electrodes, with the working electrode typically serving as a substrate. Although restricted to specific metallic elements, the process of co-deposition involves depositing multiple elemental precursors together in a single electrolyte to form either an alloy or a chemical compound. This method is commonly employed to create thin films of compounds such as sulfides, tellurides, and selenides. Electro-

deposition of metal selenides occurs in acidic conditions, typically with a pH between 1 and 3. This pH range is determined by the stability of the chemical species.

FeSe material was synthesized using electrochemical deposition, which involves reducing iron ions onto a substrate. Using this method, one can achieve accurate control of the deposition process, enabling the creation of FeSe films of exceptional quality. Electrochemical deposition offers several advantages over other synthesis methods, such as high deposition rate and controllable film thickness and morphology. It also has low cost and scalability. This study reported the enhancement of energy bandgap, structural, and electrical conductivity of electrochemically synthesized FeSe nanostructured material for photovoltaic applications.

Experimental

FeSe material was synthesized using the electrochemical deposition technique. The Iron nitrate nonahydrate ($Fe(NO_3)_2.9H_2O$) (0.1 mol) and Selenium (IV) oxide (SeO_2) (0.1 mol) are parts of the electrochemical bath system. The reaction bath was stirred using a magnetic stirrer. The electric field (DC voltage) was created by the power supply, using conducting glass for the cathode and carbon and fluorine electrodes for the anode. Finally, we have successfully achieved uniform deposition of thin films using electrochemical deposition. The working electrode, coated with FTO and measuring 2.5 cm × 1.5 cm, was fragmented and cleaned using dishwashing liquid. To create FeSe, mix 0.1 mol of $Fe(NO_3)_2.9H_2O$ and Selenium (IV) oxide (SeO_2), a three-electrode system is used in the synthesis. The anode utilizes platinum, while the reference electrode comprises silver and silver chloride (Ag/AgCl), and the cathode is made of FTO (fluorine-doped tin oxide). The counter and reference electrodes were housed vertically in the beaker on the FTO-coated substrate. The synthesis required keeping a potentiostatic condition of -200 mV versus SCE for 5 seconds. The hand dryer was used to clean and dry the synthesized films. In the synthesis process, beakers were filled with target materials and equal amounts of precursors. A 20-minute annealing treatment at 200 °C was performed on the films to ease internal stress using the muffle furnace. The synthesized materials were thoroughly analyzed using a continuous-scan X-ray diffractometer D8-Advance from Bruker, operated in locked coupled mode with Cu-Kα radiation (ʎ = 1.5406 Å). The 756S UV-Visible spectrophotometer was used to measure the absorption wavelength from 300 to 1100 nm. The absorbance values were analyzed optically to infer additional optical and solid-state features. The electrical properties of the films were analyzed using the Jandel four-point probes method.

Results

XRD Analysis

Figure 1 illustrates the crystal structures of FeSe material, as revealed by the XRD pattern.

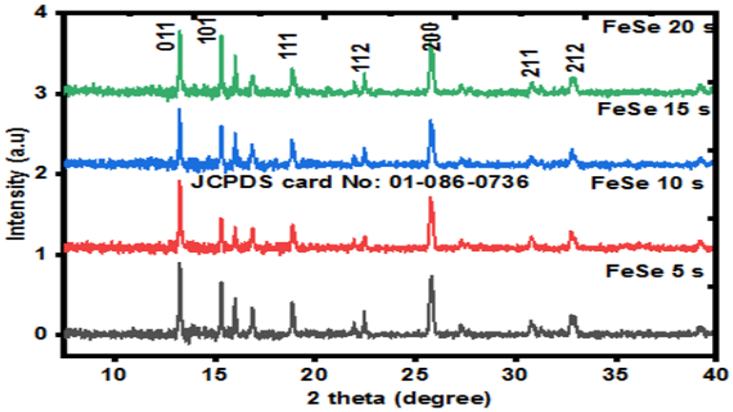

Figure 1 XRD pattern of FeSe material

FeSe material exhibits a diffraction value of 14.372o at 2θ. The diffraction peaks at 2θ = 14.372°, 15.027°, 19.112°, 23.575° 26.623° 32.292° and 34.242° correspond respectively to the diffraction planes of 011, 101, 111, 112, 200, 211, and 212 of FeSe material. The crystallite size of the electrode material was determined by applying Equation (1) [29-37].

$$D = \frac{k\lambda}{\beta cos\theta} \quad (1)$$

Where, k = 0.9, λ = 0.12406 nm (wavelength of X-ray source), and β = FWHM in radians. The calculation of the crystallite size of FeSe material is presented in Table 1. Changing the time interval (between 5 and 20 seconds) leads to modifications in the structure of FeSe material during deposition. This process influences the properties and performance of the material. The deposition time increase leads to the growth of the crystallite size in FeSe material. This indicates enhanced crystallinity

Table 1 Structural values of FeSe material

Films	2θ (degree)	d (spacing) Å	(Å)	(β)	(hkl)	(D) nm	σ lines/m² x 10^{14}
FeSe 5 s	14.372	6.161	10.672	0.112	011	1.248	1.953
	15.027	5.894	11.789	0.114	101	1.227	2.020
	19.112	4.643	9.286	0.117	111	1.202	2.105
	23.575	3.773	8.437	0.119	112	1.191	2.146
	26.623	3.347	8.200	0.121	200	1.178	2.193
	32.292	2.771	7.839	0.125	211	1.155	2.280
	34.242	2.618	7.405	0.127	212	1.143	2.330
FeSe 10 s	14.692	6.028	10.441	0.133	011	1.051	2.754
	15.121	5.858	11.716	0.135	101	1.036	2.833
	19.219	4.617	9.234	0.137	111	1.027	2.887
	23.961	3.713	8.303	0.139	112	1.019	2.929
	26.911	3.312	8.114	0.141	200	1.011	2.978
	32.617	2.744	7.763	0.143	211	1.010	2.984
	34.862	2.573	7.277	0.145	212	1.001	3.037
FeSe 15 s	14.692	6.028	10.441	0.148	011	0.945	3.411
	15.121	5.858	11.716	0.149	101	0.939	3.452
	19.219	4.617	9.234	0.152	111	0.925	3.554
	23.961	3.713	8.303	0.156	112	0.908	3.689
	26.911	3.312	8.114	0.159	200	0.896	3.787
	32.617	2.744	7.763	0.161	211	0.897	3.783
	34.862	2.573	7.277	0.163	212	0.890	3.839
FeSe 20 s	14.692	6.028	10.441	0.163	011	0.858	4.137
	15.121	5.858	11.716	0.165	101	0.848	4.233
	19.219	4.617	9.234	0.168	111	0.837	4.342
	23.961	3.713	8.303	0.169	112	0.838	4.329
	26.911	3.312	8.114	0.172	200	0.829	4.432
	32.617	2.744	7.763	0.174	211	0.830	4.419
	34.862	2.573	7.277	0.177	212	0.820	4.526

and grain growth in the material. By varying the times, the crystallite of the FeSe material is enhanced. Both the material and optical bandgap are affected by these crystallites. Crystal structure and phase composition of iron selenide vary with deposition time, as showed by XRD patterns obtained at different times (5 to 20 seconds)

Electrical Study

The investigation examined the resistivity and conductivity of FeSe thin films synthesized at various deposition times (5-20 seconds). The results showed that longer deposition time resulted in lower resistivity and higher conductivity. Depending on the deposition time, electrical properties of FeSe thin films showed significant variations. Longer deposition times reduced resistivity and an increase in conductivity, demonstrating improved electrical performance in Table 2 & Figure 2. The study proposes that by optimizing the deposition time, the electrical conductivity of FeSe thin films can be enhanced, making it essential for electronic devices and energy storage systems.

Optical Analysis

Figure 3 depicts the absorbance of FeSe material. The absorbance properties of iron selenide material differ based on deposition times ranging from 5 to 20 seconds. With increasing deposition time, the absorption of light increases, resulting in improved photovoltaic activity [38-40]. The desired properties determine the ideal time for synthesizing iron selenide material. For example, depositing the material for 10 seconds can cause a high absorption coefficient,

Table 2 Electrical properties of FeSe nanostructured material

Samples	Thickness, t (nm)	Resistivity, ρ (Ω.m) X 10^{-7}	Conductivity, σ (S/m) X 10^{-9}
FeSe 5	103.76	87.46	1.14
FeSe 10	105.09	82,98	1.21
FeSe 15	107.85	78.45	1.27
FeSe 20	109.82	69.56	1.44

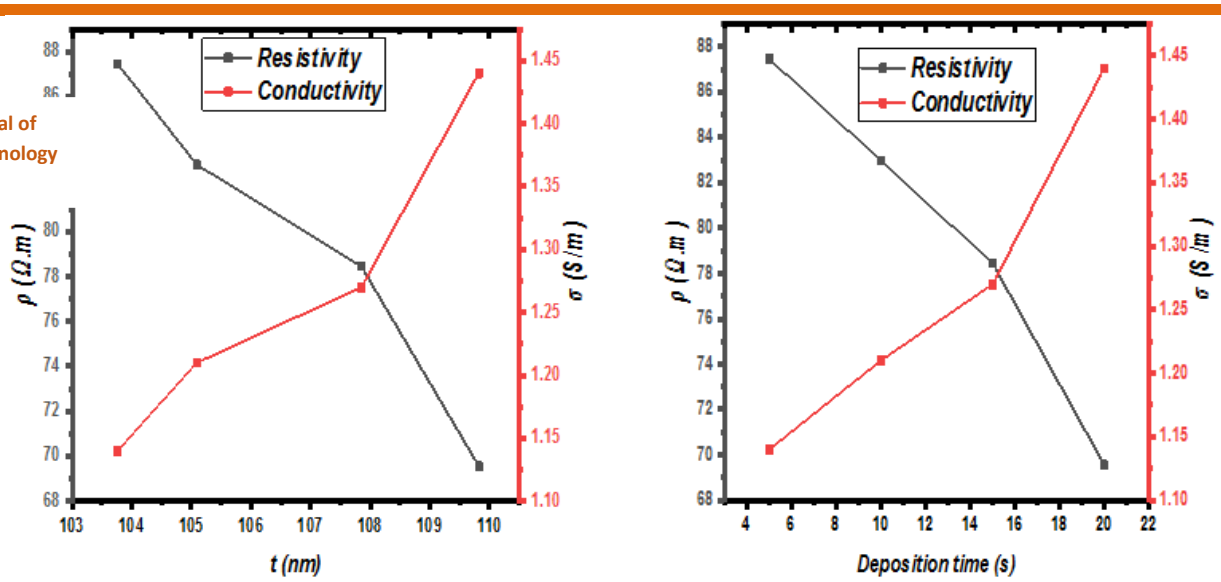

Figure 2 Resistivity and conductivity measurements for films deposited at 5s, 10s, 15s, and 20 s

whereas depositing it for 20 seconds can lead to improved crystallinity. Electrochemical deposition was used to synthesize iron selenide material. The method used for synthesis affects the properties of the material, including its crystal structure and absorption characteristics. Figure 4 demonstrates the transmittance of FeSe material. Th values of transmittance, reflectance, and bandgap values are calculated utilizing expressions in [41-43].The transmittance of iron selenide material was measured after being synthesized for various deposition times, ranging from 5 to 20 seconds. Depositing the material for 20 seconds leads to thicker films that have lower transmittance. The ideal time to deposit iron selenide varies based on the film characteristics desired. Shorter deposition times may be favored for those who prioritize deposition times may not be preferred. The chosen synthesis technique influences the transmittance and other properties of the resulting material. The films' transmittance is usually improved through the chosen synthesis techniques.

Figure 5 illustrates the reflectance of FeSe material. The electrochemical deposition method was used to deposit nanostructured FeSe thin films on glass substrates. The research examined how the films behaved optically during various deposition times. The investigation focused on the reflectance of iron selenide material synthesized within deposition times ranging from 5 to 20 seconds. The reflectance was found to rise as the deposition time increased. This is because the film becomes more compact and uniform, resulting in a higher density of crystallites. Figure 6 deisplays the bandgap energy of FeSe material. The band structure of iron selenide (FeSe) material synthesized at different deposition times between 5 and 20 seconds exhibits unique characteristics. The deposition time significantly impacts the band structure of FeSe. Longer deposition times lead to an increase in the thickness and grain size of the FeSe films, which can affect the electronic band structure. Iron selenide material showed a direct transition bandgap ranging from 2.10 to 1.65 eV at deposition times of 5 to 20 seconds.

The energy bandgap of FeSe thin films is heavily influenced by increasing the deposition time. Longer deposition times lead to a decrease in the bandgap. Several factors, such as changes in the film's microstructure, stoichiometry, and defect density, contribute to this phenomenon. Increased deposition times result in larger crystallite sizes, potentially decreasing the bandgap through reduced quantum confinement effects. The bandgap can

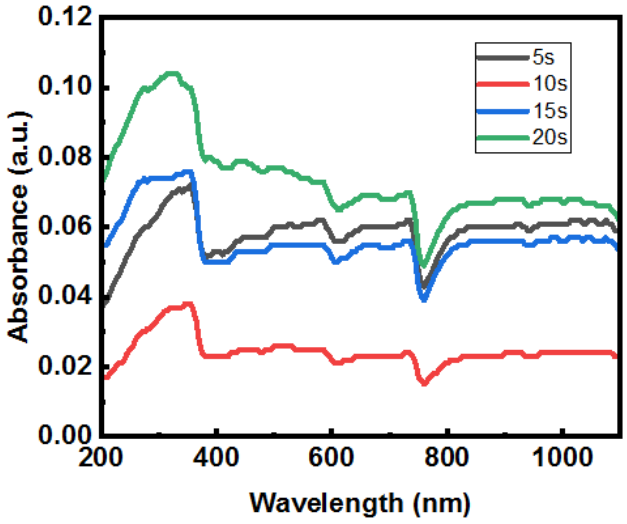

Figure 3 Absorbance curves for films deposited at 5 s, 10 s, 15 s, and 20 s

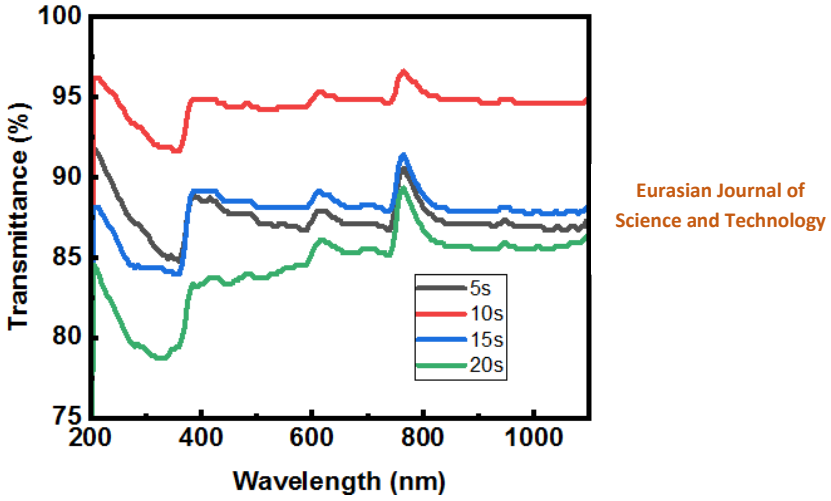

Figure 4 Transmittance curves for films deposited at 5 s, 10 s, 15 s, and 20 s

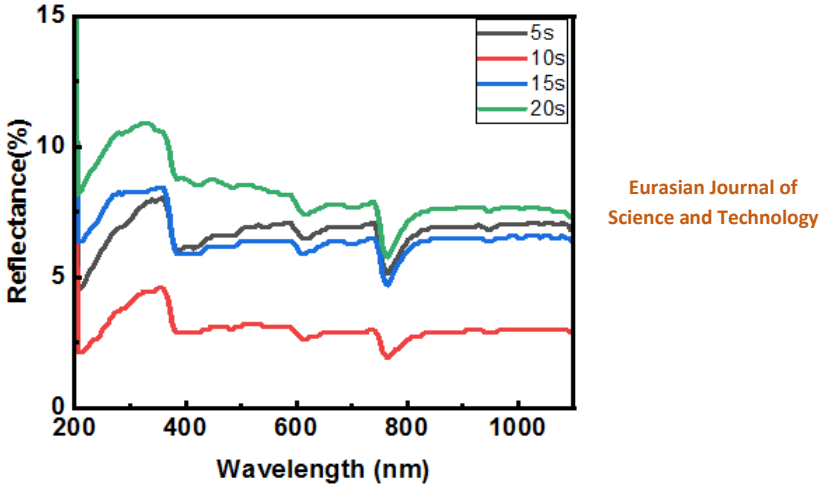

Figure 5 Reflectance curves for films deposited at 5 s, 10 s, 15 s, and 20 s

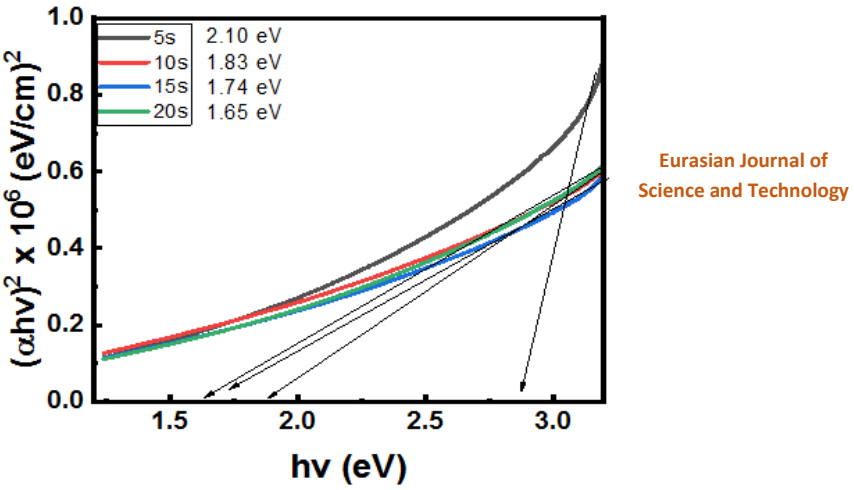

Figure 6 Bandgap curves for films deposited at 5 s, 10 s, 15 s, and 20 s

also be influenced by changes in the film's stoichiometry, like a higher Fe content. Increasing deposition times can also result in higher defect density in the film, which decreases the bandgap because of recombination centers. The suitable bandgap and high absorption coefficient of FeSe make it a promising material for solar cell applications. Optimizing the performance of FeSe-based solar cells involves tuning the bandgap. Good thermoelectric properties can also be observed in FeSe. The efficiency of FeSe-based thermoelectric devices can be improved by controlling the bandgap. The grain size of FeSe material decreased as the deposition time increased. Longer deposition times result in more atoms being deposited and forming a more ordered crystalline structure [44,45]. The energy bandgap decreases as the deposition time and crystallite size of FeSe decrease. The quantum confinement effect refers to the phenomenon where the bandgap decreases as the crystallite size increases. The correlation between deposition time and FeSe properties is vital for improving its performance in different applications. Changing the deposition time affects the conductivity, magnetic properties, and potential applications of the material, like solar cells or energy-related technologies.

Conclusion

We have successfully used the electrochemical deposition technique to synthesize FeSe material. FeSe material exhibits a diffraction value of 14.372o at 2θ. The diffraction peaks at 2θ = 14.372°, 15.027°, 19.112°, 23.575°, 26.623°, 32.292°, and 34.242° correspond, respectively, to the diffraction planes of 011, 101, 111, 112, 200, 211, and 212 of FeSe material. The results showed that longer deposition time resulted in lower resistivity and higher conductivity. Longer deposition times lead to an increase in the thickness and grain size of the FeSe films, which can affect the electronic band structure. Iron selenide material showed a direct transition bandgap ranging from 2.10 to 1.65 eV at deposition times of 5 to 20 seconds. The reflectance was found to rise as the deposition time increased. This is because the film becomes more compact and uniform, resulting in a higher density of crystallites.

The credit for the authorship is as follows: *Ernest O. Ojegu, Okpara Nathaniel and Imosobomeh L. Ikhioya:* conceptualization, methodology, Data curation, *Imosobomeh L. Ikhioya:* data collection, first-draft writing, reviewing, software, and editing**.** *Investigation and visualization:* All authors approved the submission.

Conflict of Interest

The authors declare no personal or financial conflicts that may have impacted the research in question.

Availability of data

Data can be accessed by making a request.

Acknowledgments

We extend our thanks to all the authors for their financial support, which contributed to the success of the study.

ORCID

Imosobomeh L. Ikhioya

https://orcid.org/0000-0002-5959-4427

References

[1] Rehman A.U., Munir T., Afzal S., Saleem M., Ikhioya I.L., Enhanced solar cell efficiency with tin-based lead-free material ($FASnI_3$) through SCAPS-1D modeling, *Eurasian Journal of Science and Technology*, 2024, **4**: 244 [Crossref], [Publisher]

[2] JBai J., Wu H., Wang S., Zhang G., Feng C. Synthesis and electrochemical performances of $FeSe_2$/C as anode material for lithium ion batteries, *Journal of Electronic Materials*, 2019, **48**:5933 [Crossref], [Google Scholar], [Publisher]

[3] Demura S., Okazaki H., Ozaki T., Hara H., Kawasaki Y., Deguchi K., Watanabe T., Denholme S.J., Mizuguchi Y., Yamaguchi T. Electrodeposition as a new route to synthesize superconducting FeSe, *Solid State Communications*, 2013, **154**:40 [Crossref], [Google Scholar], [Publisher]

[4] Demura S., Tanaka M., Yamashita A., Denholme S.J., Okazaki H., Fujioka M., Yamaguchi T., Takeya H., Iida K., Holzapfel B. Electrochemical deposition of FeSe on RABiTS tapes, *Journal of the Physical Society of Japan*, 2016, **85**:015001 [Crossref], [Google Scholar], [Publisher]

[5] Huang Y., Ren S. Controlled growth and chemical engineering of FeSe-based superconducting films, *Advanced Physics Research*, 2023, **2**:2200058 [Crossref], [Google Scholar], [Publisher]

[6] Hussain A., Ali F., Ahmed H.H., Ikhioya I.L. Enhanced specific capacitance, structural, optical, and morphological study of carbon ions incorporated into the lattice of $ZrCuO_2$ nanoparticle synthesized by hydrothermal method, *Hybrid Advances*, 2024, **5**:100170 [Crossref], [Google Scholar], [Publisher]

[7] Ikhioya I.L., Nkele A.C., Okoro C.F., Obasi C., Whyte G.M., Maaza M., Ezema F.I., Effect of temperature on the morphological, structural and optical properties of electrodeposited Yb-doped $ZrSe_2$ thin films, *Optik*, 2020, **220**:165180 [Crossref], [Google Scholar], [Publisher]

[8] Ikhioya I.L., Nkele A.C. Green synthesis and characterization of aluminum oxide nanoparticle using neem leaf extract (Azadirachta Indica), *Hybrid Advances*, 2024, **5**:100141 [Crossref], [Google Scholar], [Publisher]

[9] Ke J., Zhang R., Zhang P., Yu R., Cao X., Kuang P., Wang B., Investigation on structural and optical properties of ZnSe thin films prepared by selenization, *Superlattices and Microstructures*, 2021, **156**:106965 [Crossref], [Google Scholar], [Publisher]

[10] Li S., Li D., Jiang J., Liu G., Ma S., Liu W., Zhang Z. Growth process and magnetic properties of α-FeSe nanostructures, *Journal of Applied physics*, 2014, **115** [Crossref], [Google Scholar], [Publisher]

[11] Mishra S., Song K., Koza J.A., Nath M. Synthesis of superconducting nanocables of FeSe encapsulated in carbonaceous shell, *ACS Nano*, 2013, **7**:1145 [Crossref], [Google Scholar], [Publisher]

[12] Nnannaa L.A., Jospeh U., Nwaokorongwu E.C., U. A E., Akpu N.I., Ikhioya I.L. Impact of annealing temperature on praseodymium cerium telluride nanoparticles synthesise via hydrothermal approach for optoelectronic application, *Materials Research Innovations*, 2024, 1 [Crossref], [Google Scholar], [Publisher]

[13] Pawar S., Moholkar A., Suryavanshi U., Rajpure K., Bhosale C. Electrosynthesis and characterization of iron selenide thin films, *Solar Energy Materials and Solar Cells*, 2007, **91**:560 [Crossref], [Google Scholar], [Publisher]

[14] Piperno L., Celentano G., Sotgiu G. Electrodeposition of iron selenide: a review, *Coatings*, 2023, **13**:1905 [Crossref], [Google Scholar], [Publisher]

[15] Rufus I., Ikhioya I.L. Enhanced electrical, morphology, structural, and optical features of nickel silver sulphide material for photovoltaic applications, 2023, **11**:1 [Crossref], [Google Scholar]

[16] Ubale A., Sakhare Y., Belkedkar M., Singh A. Characterization of nanostructured iron selenide thin films grown by chemical route at room temperature, *Materials Research Bulletin*, 2013, **48**:863 [Crossref], [Google Scholar], [Publisher]

[17] Zhang H., Long G., Li D., Sabirianov R., Zeng H. Fe3Se4 nanostructures with giant coercivity synthesized by solution chemistry, *Chemistry of Materials*, 2011, **23**:3769 [Crossref], [Google Scholar], [Publisher]

[18] Ogonnaya O.C. The Influence of precursor temperature on the properties of erbium-doped zirconium telluride thin film material via electrochemical deposition, *Int. J. Appl. Phys.*, 2020, 102 [Crossref], [Google Scholar]

[19] Francsic O.I., Ikhioya I.L., Effect of sodium arsenic on the improvement of TiO_2/ dye as photosensitizers in dye-sensitized solar cells (DSSC), *Asian Journal of Green Chemistry*, 2024, **8**:137 [Crossref], [Google Scholar], [Publisher]

[20] Obitte B.C.N., Ikhioya I.L., Whyte G.M., Chime U.K., Ezekoye B.A., Ekwealor A.B.C., Maaza M., Ezema F.I., The effects of doping and temperature on properties of electrochemically deposited Er^{3+} doped ZnSe thin films, *Optical Materials*, 2022, **124**:111979 [Crossref], [Google Scholar], [Publisher]

[21] Ikhioya I.L., Onoh E.U., Okoli D.N., Ekpunobi A.J. Impact of bismuth as dopant on ZnSe material syntheses for photovoltaic application, *Materials Research Innovations*, 2023, **27**:411 [Crossref], [Google Scholar], [Publisher]

[22] Ikhioya I.L., Aisida S.O., Ahmad I., Ezema F.I. The effect of molybdenum dopant on rare earth metal chalcogenide material, *Chemical Physics Impact*, 2023, **7**:100269 [Crossref], [Google Scholar], [Publisher]

[23] Ikhioya I.L., Nkele A.C. Properties of electrochemically-deposited NiTe films doped with molybdenum at varying temperatures, *Results in Optics*, 2023, **12**:100494 [Crossref], [Google Scholar], [Publisher]

[24] Ikhioya I.L., Nkele A.C. A novel synthesis of hydrothermally-prepared yttrium selenide and erbium selenide nanomaterials doped with magnesium, *Results in Optics*, 2023, **13**:100555 [Crossref], [Google Scholar], [Publisher]

[25] Okeoghene Blessing I., Shah H., Afzal S., Ikhioya I.L. Enhanced structural properties of electrochemically synthesised NiFeS using 500 keV carbon C++ ions irradiation, *Materials Research Innovations*, 2023, 1 [Crossref], [Google Scholar], [Publisher]

[26] Ojegu E.O., Samuel S.O., Osiele M.O., Akpojotor G.E., Ikhioya I.L. Optimisation of deposition voltage of zirconium-doped chromium telluride via typical three-electrode cell electrochemical deposition technique, *Materials Research Innovations*, 2024, **28**:137 [Crossref], [Google Scholar], [Publisher]

[27] Sengar M., Saxena S., Satsangee S., Jain, R., Silver nanoparticles decorated functionalized multiwalled carbon nanotubes modified screen printed sensor for the voltammetric determination of butorphanol, *Journal of Applied Organometallic Chemistry*, 2021, **1**:95 [Crossref], [Google Scholar], [Publisher]

[28] Malumi S.O., Malumi T., Osiele M.O., Ekpekpo A., Ikhioya I.L. Enhance and performance evolution of silver-doped titanium dioxide dye-sensitized solar cells using different dyes, *Journal of Engineering in Industrial Research*, 2023, **4**:189 [Crossref], [Google Scholar], [Publisher]

[29] Sarwar S.G., Ikhioya I.L., Afzal S., Ahmad I. Supercapitance performance evaluation of MXene/Graphene/NiO composite electrode via in situ precipitation technique, *Hybrid Advances*, 2023, **4**:100105 [Crossref], [Google Scholar], [Publisher]

[30] Samuel S.O., Frank M.L.-e., Ogherohwo E., Ekpekpo A., Zhimwang J., Ikhioya I.L. Influence of deposition voltage on strontium sulphide doped silver for optoelectronic application, *East European Journal of Physics*, 2023, 189 [Crossref], [Google Scholar], [Publisher]

[31] Samuel S.O., Lagbegha-ebi M.F., Ogherohwo E., Ikhioya I.L. Improve physical properties of zirconium doped strontium sulphide for optoelectronic purpose, *Results in Optics*, 2023, **13**:100518 [Crossref], [Google Scholar], [Publisher]

[32] Samuel S.O., Ojoba C.K., Ogherohwo E., Ojegu E.O., Zhimwang J., Ekpekpo A., Ikhioya I.L. The influence of precursor temperature on strontium sulphide doped silver for optoelectronic application, *Journal of the Indian*

Chemical Society, 2023, **100**:100992 [Crossref], [Google Scholar], [Publisher]

[33] Samuel S.O., James F.E., JT Z., EP O., Ekpekpo A., Ikhioya I.L. Effect of dopant on the energy bandgap on strontium sulphide doped silver for optoelectronic application, *Materials Research Innovations*, 2024, **28**:8 [Crossref], [Google Scholar], [Publisher]

[34] Samuel S.O., Timothy Z.J., Ojoba C.K., Ikhioya I.L. Temperature's impact on the physical properties of rare earth element doped SrS for optoelectronic use, *Journal of Engineering in Industrial Research*, 2023, **4**:147 [Crossref], [Google Scholar], [Publisher]

[35] Udofia K., Lucky I. Electrical Properties of Electrodeposited Lead Selenide (PbSe) Thin Films, *Asian Journal of Physical and Chemical Sciences*, 2018, **5**:1 [Crossref], [Google Scholar], [Publisher]

[36] Ibrar S., Zafar Ali N., Ojegu E. O., Odia O. B., L. Ikhioya I., Ahmad I., Assessing high-performance energy storage of the synthesized ZIF-8 and ZIF-67, *Journal of Applied Organometallic Chemistry*, 2023, **3**:294 [Crossref], [Google Scholar], [Publisher]

[37] Udofia, K.I., Ikhioya, I.L., Okoli, D.N., Ekpunobi A.J., Impact of solution pH on the physical properties of rare earth metal doped PbSe chalcogenide material for photovoltaic application, *Journal of Engineering in Industrial Research*, 2023, **4**:157 [Crossref], [Google Scholar], [Publisher]

[38] Raveendran N.R., Kumary T.G., Rajkumari S., Pandian R., Janaki J., Mani A.: Synthesis and study of FeSe thin films and $LiFeO_2$/FeSe bi-layers, *AIP Conference Proceedings:* 2017 [Crossref], [Google Scholar], [Publisher]

[39] Qiu W., Ma Z., Patel D., Sang L., Cai C., Shahriar Al Hossain M., Cheng Z., Wang X., Dou S.X. The interface structure of FeSe thin film on CaF_2 substrate and its influence on the superconducting performance, *ACS applied materials & interfaces*, 2017, **9**:37446 [Crossref], [Google Scholar], [Publisher]

[40] Imai Y., Sawada Y., Nabeshima F., Asami D., Kawai M., Maeda A. Control of structural transition in FeSe1−x Te x thin films by changing substrate materials, *Scientific Reports*, 2017, **7**:46653 [Crossref], [Google Scholar], [Publisher]

[41] Ikhioya I.L., Ali N.Z., Tahir S., Afzal S., Shah A., Ahmad I., Ezema F.I. Electrochemical engineering of ZIF-7 electrode using ion beam technology for better supercapacitor performance, *Journal of Energy Storage*, 2024, **90**:111833 [Crossref], [Google Scholar], [Publisher]

[42] Okeoghene Blessing I., Shah H., Afzal S., Ikhioya I.L. Enhanced structural properties of electrochemically synthesised NiFeS using 500 keV carbon C++ ions irradiation, *Materials Research Innovations*, 2023, 1 [Crossref], [Google Scholar], [Publisher]

[43] Shah H., Afzal S., Usman M., Shahzad K., Ikhioya I. Impact of annealing temperature on lanthanum erbium telluride (La0. 1Er0. 2Te0. 2) nanoparticles synthesized via hydrothermal approach, *Advanced Journal of Chemistry, Section A*, 2023, **6**:342 [Crossref], [Google Scholar], [Publisher]

[44] El-Shaer A., Ezzat S., Habib M.A., Alduaij O.K., Meaz T.M., El-Attar S.A. Influence of deposition time on structural, morphological, and optical properties of CdS thin films grown by low-cost chemical bath deposition, *Crystals*, 2023, **13**:788 [Crossref], [Google Scholar], [Publisher]

[45] Mohammed K.A., Ahmed S.M., Mohammed R.Y. Investigation of structure, optical, and electrical properties of CuS thin films by CBD technique, *Crystals*, 2020, **10**:684 [Crossref], [Google Scholar], [Publisher]